American Mineralogist, Volume 73, pages 741–753, 1988

Cr-rich spinels as petrogenetic indicators: MORB-type lavas from the Lamont seamount chain, eastern Pacific

James F. Allan*
Department of Geological Sciences, Northwestern University, Evanston, Illinois 60201, U.S.A.

Richard O. Sack
Department of Earth and Atmospheric Sciences, Purdue University, West Lafayette, Indiana 47907, U.S.A.

Rodey Batiza
Department of Geological Sciences, Northwestern University, Evanston, Illinois 60201, U.S.A.

Abstract

The composition and morphology of Cr-rich spinels in MORBs reflect and record pre-eruptive petrogenetic events such as magma-chamber recharge, fractionation, and magma mixing. In this paper we examine Cr-rich spinels in MORB-type lavas erupted from the near-ridge Lamont seamounts and from the adjacent East Pacific Rise crest at 10°N. The spinels studied are exclusively from quickly quenched glassy to spherulitic flow margins. The host lavas are depleted [$(La/Sm)_N < 0.57$] and relatively primitive [$Mg/(Mg + Fe^{2+})$ to 0.71, Cr to 460 ppm], with the most primitive samples approaching the composition of liquids in equilibrium with mantle peridotite. The spinels cover a wide range in Al and Cr contents, with spinel $Cr/(Cr + Al)$ ranging from 0.20 to 0.54 for the entire suite. As in other depleted MORBs, TiO_2 and calculated Fe_2O_3 contents in the spinels are low (0.16–0.85 and 5.5–9.2 wt%, respectively). Contents of Al, Mg, and Fe of groundmass spinels strongly correlate with host-glass composition, but spinel Cr content shows little correlation with host-glass Cr content. Casting of spinel compositions in terms of $Mg\text{-}Fe^{2+}$ spinel–host liquid exchange equilibria and in terms of the compositionally related crystallochemical effects on this exchange shows that for a given lava suite derived from similar parental lavas, spinel $Cr/(Cr + Al)$ increases and $Mg/(Mg + Fe^{2+})$ decreases with the amount of Fe enrichment, Al depletion, and extent of fractionation [as represented by the normative ratio Diop/(Ol + Diop)] of the liquids in which they equilibrated. This change in spinel composition is of much greater magnitude than that of the host liquid; thus spinels are sensitive indicators of melt composition and crystal-liquid equilibrium and disequilibrium processes. MORB lavas containing strongly zoned spinels or populations of spinels with broad compositional range preserve direct evidence of host-melt prehistory of interaction with other melts (magma mixing) or other processes such as wall-rock interaction. The strong compositional covariance of Cr-rich spinel and host silicate liquid makes the formulation of a spinel geobarometer difficult.

Introduction

Cr-rich spinel within MORB-like lavas has long been acknowledged as carrying useful information regarding the petrogenesis of its host lavas. Although the crystal chemistry and thermochemistry of spinels are complex (e.g., Sack, 1982; Irvine, 1976), the composition of spinel is a sensitive indicator of magmatic intensive and extensive variables (Irvine, 1965, 1967). Inferences regarding magma mixing (Natland et al., 1983) and initiation of precipitation of coexisting phases (Fisk and Bence, 1980; Foruta and Tokuyama, 1983; Dick and Bullen, 1984) have been made from variations in MORB Cr-spinel compositions. MORB spinel chemistry has also been used to deduce information about magmatic intensive variables, including pressure (Sigurdsson and Schilling, 1976; Sigurdsson, 1977; Dick and Bryan, 1978; Dick and Bullen, 1984), f_{O_2} (Fisk and Bence, 1980; Batiza and Vanko, 1984) and temperature (Fisk and Bence, 1980) during crystallization. We consider here systematic changes in spinel composition among Cr-rich spinels from basalts erupted along the Lamont seamount chain, a group of seamounts near the axis of the East Pacific Rise (EPR) occurring west of the EPR at 10°N, just south of the Clipperton Fracture Zone (Fig. 1), and within Cr-rich spinels from lavas erupted at the EPR axis at 10°N. Samples were collected in situ from sheet and lobated flows, pillows, massive

* Present address: Department of Geological Sciences, University of British Columbia, Vancouver, British Columbia V6T 2B4, Canada.

0003–004X/88/0708–0741$02.00

TABLE 1. Glass analyses of spinel-bearing lavas

Location:*	Cone near MOK	Cone near SASHA				DTD 1572-1511	DTD 1572-1755	EPR 1567-1816	EPR 1567-2019	MIB 1560-1843
Sample:	F9-1	F1-1	F2-1	F2-2	F3-4					
SiO_2	49.60	50.41	48.40	48.79	48.81	48.68	48.96	50.06	49.87	49.32
TiO_2	1.21	1.18	0.86	0.83	0.83	1.01	1.14	1.16	1.20	1.36
Al_2O_3	16.85	15.49	17.38	17.50	17.91	17.64	16.88	16.21	16.03	16.99
Fe_2O_3	0.84	1.23	0.81	0.86	1.02	0.89	0.99	0.89	1.02	0.95
FeO	7.83	8.19	7.60	7.45	7.48	7.59	7.94	8.01	8.18	8.09
MgO	8.97	8.14	9.44	9.50	9.53	9.10	8.51	8.28	8.28	7.84
CaO	12.35	13.00	13.16	12.87	12.90	12.45	12.28	12.47	12.70	11.95
Na_2O	2.46	2.41	2.18	2.13	2.08	2.65	2.71	2.46	2.44	3.34
K_2O	0.10	0.06	0.02	0.02	0.01	0.03	0.06	0.11	0.09	0.04
P_2O_5	0.10	0.11	0.07	0.09	0.09	0.08	0.13	0.14	0.14	0.14
Total	100.31	100.22	99.92	100.04	99.94	100.12	99.60	99.79	99.95	100.02
$Mg/(Mg + Fe^{2+})$	0.671	0.639	0.689	0.694	0.694	0.681	0.656	0.648	0.643	0.633
Sc	35.5	39.9	31.1	31.7	32.3	28.7	35.4	38.1	38.2	37.0
Cr	430	400	460	440	370	290	330	350	360	280
Co	46.8	44.5	50.0	48.0	48.8	40.3	47.0	43.3	43.6	43.9
Ni	190	120	240	210	200	160	140	160	110	120
La	2.76	2.04		0.92	0.88	1.20	1.83	2.67	2.71	2.81
Yb	2.24	2.39	1.81	1.91	1.91	1.64	2.34	2.49	2.54	2.66
Hf	2.06	1.75	1.28	1.29	1.19	1.46	1.88	2.07	2.06	2.60
$(La/Sm)_N$	0.57	0.47		0.28	0.27	0.34	0.40	0.55	0.57	0.47

Note: Major elements analyzed by electron microprobe at the Smithsonian Institution (T. O'Hearn, analyst). Trace elements (in ppm) analyzed by INAA at Washington University, St. Louis, Missouri, and reported from Allan et al. (submitted manuscript; see footnote 1 in text); analytical precision discussed in Allan et al. (1987). FeO measured by I.S.E. Carmichael, using wet-chemical methods; Fe_2O_3 calculated by difference from FeO_T, as measured by T. O'Hearn. $Mg/(Mg + Fe^{2+})$ calculated for 1560-1843 and 1572-1511 assuming $Fe^{2+}/(Fe^{2+} + Fe^{3+}) = 0.904$, the average value for the other analyzed lavas. $(La/Sm)_N$ represents La and Sm values normalized to chondritic values (Haskin et al., 1968).

* See Figure 1.

flow interiors, and talus slopes by the *ALVIN* submersible and by dredging.

The seamounts are associated with a broad, topographic high at the adjacent EPR, interpreted as representing recent voluminous ridge volcanism (Gallo et al., 1986; Kastens et al., 1986). The EPR at this latitude is apparently underlain by a magma chamber (Detrick et al., 1987). All seamounts show signs of recent volcanic activity, based on the youthful appearance of flow surfaces, lack of sediment cover, and absence of thick ferro-manganese coatings on surface rocks (Fornari et al., 1988a). This 50-km-long chain consists of five 1000- to 1400-m-high seamounts, with volumes ranging from 25 to 120 km^3, and most with summit craters and calderas (Fornari et al., 1984). The seamounts in turn are surrounded by abundant, 100- to 200-m-high lava cones (Fornari et al., 1988a). The chain has formed on crust of 0.1–0.74 Ma in age. The absolute age of the seamounts is unknown, but an upper limit is provided by the age of the underlying seafloor.

PETROGRAPHY AND PETROLOGY OF HOST LAVAS

The spinels occur within basalts of LREE-depleted N-type MORBs (Sun et al., 1979), with Na_2O varying from 2.1 to 3.3% and $(La/Sm)_N$ varying from 0.25 to 0.57. Other incompatible major elements and high-field-strength elements are similarly low (e.g., TiO_2, 0.81–1.43%; K_2O, <0.11%; Hf, 1.19–2.69 ppm; see Table 1). The Lamont seamounts and cones have erupted an unusual percentage of high-MgO lavas (60% are higher than 8% MgO, average MgO is 8.24%), some of which are quite primitive [MgO to 9.74%, $Mg/(Mg + Fe^{2+})$ to 0.70, Cr to 460 ppm, Ni to 240 ppm; olivines having mantle peridotite compositions of Fo_{91} to Fo_{88}; Tables 1 and 2] and could approximate primary mantle melts (Green, 1971; Frey et al., 1978; Sato, 1977; Rhodes and Dungan, 1979; Presnall et al., 1979). In contrast, the adjacent EPR lavas average 7.57% MgO (Allan et al., 1986; Langmuir et al., 1986). All spinel-bearing lavas have $Mg/(Mg + Fe^{2+})$ greater than 0.61 and contain greater than 280 ppm Cr. Analyses of glasses from spinel-containing lavas considered here are given in Table 1, and summaries of mineral compositional data for these lavas are given in Table 2. The glass analyses are considered to represent close compositional approximations of the eruptive host magmas (Melson et al., 1976; Byerly et al., 1976). Normative compostions of these glasses are plotted in Figure 2 in terms of normative Ol, Di, and Neph projecting from plagioclase, using the algorithms of Sack et al. (1987). Allan et al. (submitted manuscript)[1] show that the most primitive glass samples approximate liquids in equilibrium with peridotite at pressures of 9–9.5 kbar and solidus temperatures of 1180–1240 °C, but Figure 2 shows that most have undergone fractionation or re-equilibration at pressures of less than 9 kbar.

[1] Allan, J.F., Batiza, R., Perfit, M.R., Fornari, D.J., and Sack, R.O. Petrology of lavas from the Lamont seamount chain, Eastern Pacific: Seamount lavas as mantle probes for understanding MORB petrogenesis. Submitted to Journal of Petrology.

TABLE 1—*Continued*

MIB 1560-1922	MIB 1566-1642	MOK 1564-1857	MOK 1564-1949	MOK 1570-1949
49.09	50.07	48.94	48.55	49.42
1.43	1.17	0.96	0.94	0.96
16.50	15.14	17.02	16.92	16.60
1.02	0.91	0.83	0.97	0.89
8.07	8.86	8.07	8.23	8.03
7.80	7.81	9.18	9.24	8.78
11.81	12.71	12.80	12.88	12.67
3.31	2.60	2.30	2.26	2.43
0.04	0.04	0.04	0.04	0.04
0.17	0.13	0.12	0.14	0.08
99.24	99.44	100.26	100.17	99.90
0.633	0.611	0.670	0.667	0.661
38.0	42.9	35.6	35.3	36.0
300	380	360	360	340
43.4	45.7	50.0	49.0	47.4
100	90	80	90	140
2.87	1.54	1.24	1.59	0.99
2.71	2.71	2.08	2.08	2.27
2.69	1.81	1.40	1.42	1.48
0.47	0.33	0.33	0.43	0.26

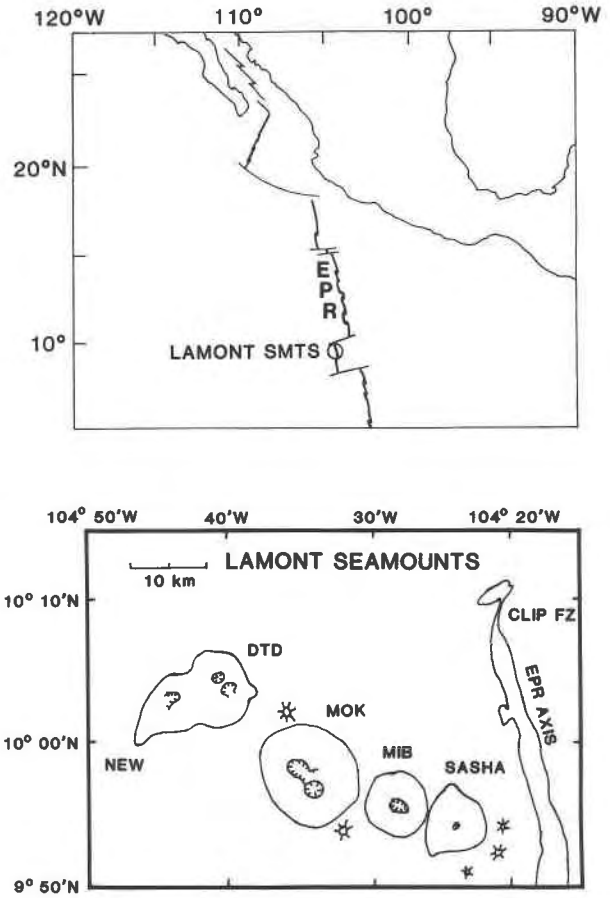

Fig. 1. Maps showing location and detail of the Lamont seamount chain. General location map after Fig. 1 of Sempere and Macdonald (1986) shows trace of East Pacific Rise and location of the seamount chain at 10°N, just south of the Clipperton Fracture Zone (FZ). Seamount map derived from SEABEAM charts (after Fornari et al., 1988a).

$^{87}Sr/^{86}Sr$ ranges from 0.702 218 to 0.702 671 within the seamount lavas; the adjacent EPR lavas have a much more restricted range of $^{87}Sr/^{86}Sr$ ratios (0.702 499–0.702 780; Perfit et al., 1986; Klein et al., 1986; Fornari et al., 1988b). Calculated eruptive temperatures (based on the crystal-liquid geothermometers of Glazner, 1984) range from 1180 to 1220 °C. Allan et al. (1986) demonstrated from sample LREE and major-element contents that the seamount lavas bypassed subaxial magma chambers thought extant at the adjacent EPR. A fuller treatment of the petrology of the Clipperton seamount lavas is given in Allan et al. (submitted manuscript; see footnote 1).

The spinel-bearing seamount and cone lavas from the Lamont seamount chain have a very simple mineralogy (Allan et al., 1986, and submitted manuscript). Most samples contain both plagioclase and olivine as phenocrysts. Samples range from nearly aphyric to porphyritic (up to 15% phenocrysts) with glomeroporphyritic clusters of plagioclase and olivine commonly present. Plagioclase phenocrysts are typically euhedral with sharp, nonscalloped outlines and may exceed several millimeters in size. Olivine phenocrysts are commonly skeletal and can be equally large. In most cases, both minerals are compositionally unzoned, with crystals rarely exhibiting any reverse zoning or normal zoning greater than 1–2 mol%. Nevertheless, exceptions do occur. Lava samples from one of the cones (F2-1 and F2-2) contain two types of olivine phenocrysts—skeletal, unzoned olivines of Fo_{89-90} composition and subhedral-euhedral, reversely zoned olivines with Fo_{87-88} cores and Fo_{89-90} rims. Minor (<1% Fo) reverse zoning is found in a few of the olivines within the lava sample 1564–1949 from the MOK seamount; its plagioclase phenocrysts exhibit oscillatory zoning as well.

Clinopyroxene is typically absent, particularly in the more primitive lavas (MgO > 8%). This absence of clinopyroxene indicates that it is not generally on the low-pressure liquidus at the pre-eruption temperatures of the Lamont seamount magmas. Indeed, most lavas from individual seamounts broadly define olivine + plagioclase fractionation-control lines in MgO variation diagrams, consistent with modeling results using least-squares mixing and with petrographic evidence (Allan et al., submitted manuscript; see footnote 1). Crystals of titanomagnetite are absent in most samples and are always <5 μm in size. Xenoliths are absent.

Spinel is often abundant in these samples (some 2.3 × 4.6 cm, 0.07-mm-thick thin sections may contain over 50 spinel grains, though this is ≪0.1% by volume) and forms translucent, light brown crystals up to 200 μm in

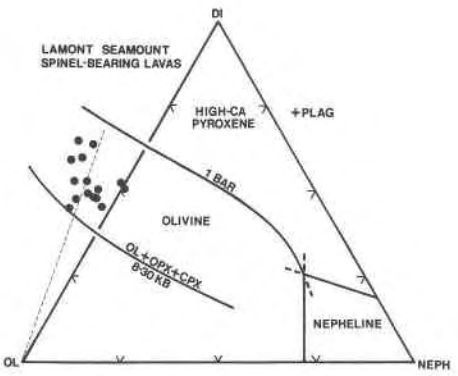

Fig. 2. Comparison of ratios of nepheline (Neph), olivine (Ol), and high-Ca pyroxene (Di) normative components of spinel-bearing Lamont seamount lavas with those for the 1-atm ($f_{O_2} \approx$ QFM) plagioclase-saturated cotectics and the high-pressure olivine + orthopyroxene + high-Ca pyroxene cotectic as defined by Sack et al. (1987). Normative components employed in this and subsequent figures are calculated from the algorithms given in Sack et al. (1987, caption to Fig. 5). Most spinel-bearing lavas are seen to have evolved at pressures less than 8 kbar by fractionation or re-equilibration, putting absolute limits on pressures of spinel precipitation. Dashed line represents an average chord emanating from the olivine vertex, representing olivine + plagioclase fractionation.

size that are found as groundmass grains, as inclusions in olivine and plagioclase, or as grains accreted to or embedded into olivine and plagioclase. The spinels encompass a wide range of shapes and include both euhedral and skeletal shapes, the latter perhaps indicative of rapid growth (Fig. 3). Curiously, the abundance of spinel in the lavas is independent of host-rock Cr content, and Cr-rich spinel has been found in samples with Cr content varying from 280 to 460 ppm (Table 1). Wide-beam (50 μm) glass microprobe analyses of long counting time (200 s) agree with mass-balance calculations based on spinel abundance that the great to overwhelming majority of magma Cr content (typically much greater than 99%) is contained within glass (representative of the host liquid) instead of within the spinels. Rock textures for all spinel-bearing lavas indicate that crystallization of spinel preceded and overlapped with the onset of olivine and plagioclase crystallization. Indeed, the experiments of Fisk and Bence (1980) show that the onset of spinel crystallization in MORBs is only tens of degrees celsius before olivine.

The simple mineralogy, the abundance of spinel, and the primitive, depleted nature of the basalts from the Lamont seamount chain suggest that the melts have had a simple ascent and eruption history. The absence of xenocrysts and xenoliths and the unzoned nature of the phenocrysts implies that most of the lavas have undergone little or no magma mixing or significant crustal assimilation. The absence of clinopyroxene in most of the lavas indicates that these lavas spent little time cooling in shallow crustal magma chambers (Walker et al., 1979), but instead underwent relatively rapid ascent. As a result, these seamount and cone lavas are good candidates to study how spinel composition is related to host-lava composition and paragenesis.

It is crucial to note that the spinels studied here are exclusively from the glassy to spherulitic and finely microlitic margins of flows, where the quenching of the lava by cool seawater during eruption was rapid to nearly instantaneous (seconds to minutes). Many of the groundmass spinels are completely surrounded by crystal-free glass. Therefore, problems with interpretation of posteruptive or syneruptive spinel growth or re-equilibration are avoided. Indeed, these lavas represent perhaps nature's closest approximation to quench conditions obtainable in the laboratory.

Spinel chemistry

The Cr-rich spinels in this study are classified as chromium spinels or magnesiochromites, using the criteria and terminology of Sigurdsson (1977). They are plotted

Table 2. Mineralogical data for lavas with Cr-rich spinel

Sample analyzed	Sample Ol Fo range	Sample Plag An range	Spinel			No. of analyses
			Cr/(Cr + Al)	Mg/(Mg + Fe^{2+})	Fe^{3+}/(Cr + Al + Fe^{3+})	
F-1-1	86–87	70–74	0.53–0.54	0.67–0.68	0.098–0.106	4
F2-1	89–90	78–89	0.20–0.50	0.75–0.84	0.056–0.075	29
F2-2	87–90	78–91	0.22–0.51	0.75–0.84	0.058–0.089	29
F3-4	89–90	76–90	0.27–0.46	0.70–0.81	0.060–0.085	20
F9-1	89–91	—*	0.35–0.41	0.73–0.78	0.069–0.084	12
1560-1843	87	61–81	0.41–0.43	0.69–0.71	0.096–0.100	4
1560-1922	86–87	66–81	0.39–0.40	0.71	0.094–0.097	2
1564-1857	—*	78–91	0.30	0.80	0.078	1
1564-1949	88	75–91	0.23–0.36	0.75–0.84	0.062–0.083	7
1566-1642	85–86	75–84	0.50–0.54	0.66–0.70	0.100–0.118	21
1567-1816	86–87	69–80	0.46–0.47	0.71–0.72	0.091–0.097	4
1567-2019	78–88	70–83	0.46–0.47	0.69–0.72	0.094–0.100	5
1570-1949	88.00	79–89	0.38–0.39	0.74–0.77	0.083–0.101	6
1572-1511	85–89	69–88	0.30–0.32	0.80–0.81	0.071–0.077	6
1572-1755	87–89	65–87	0.37–0.41	0.73–0.75	0.607–0.086	11

Note: Ranges in plagioclase, olivine, and spinel composition observed in spinel-bearing samples.
* Samples lacking either olivine or plagioclase.

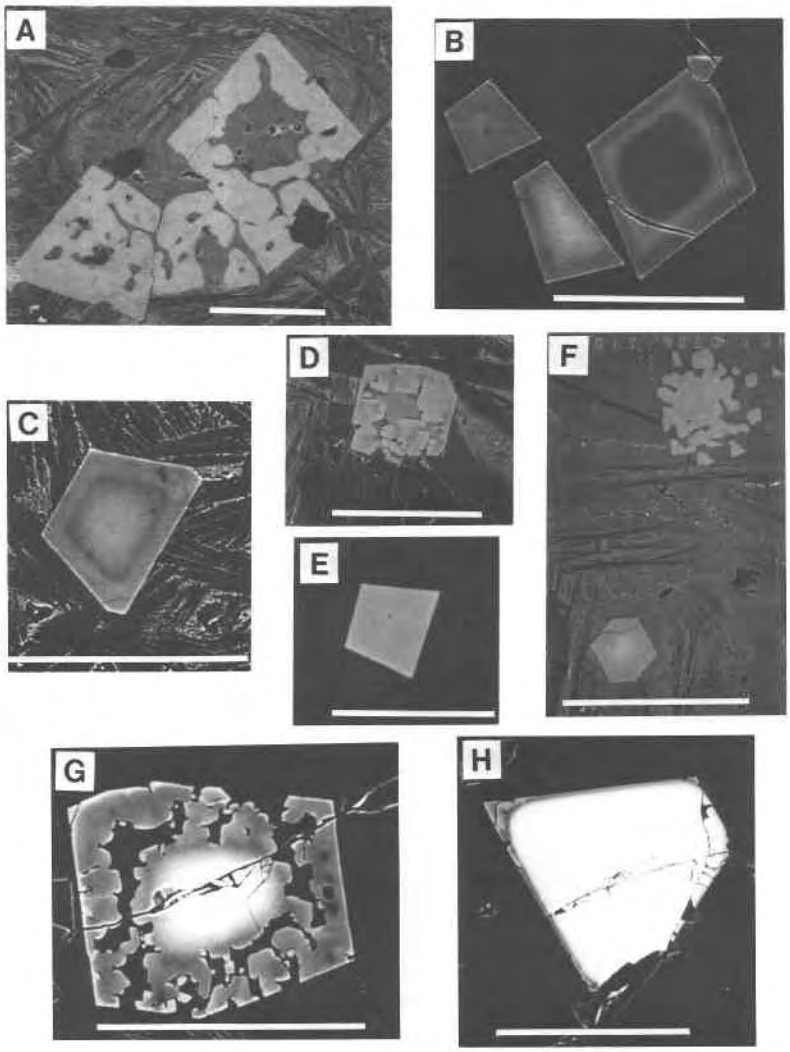

Fig. 3. Backscattered images of selected spinels, with accompanying scale bar representing 100 μm in length. Dark areas represent Al-rich regions of spinel (smaller mean atomic number), and light areas represent Cr-rich regions of spinel. Thin bright lines outlining some of the spinels are caused by edge effects. (**A**) Skeletal, relatively unzoned spinels in groundmass of plagioclase microlites and mesostasis in sample F3-4, represented by analysis of F3-4-18 in Table 3. (**B**) Complexly zoned spinels in the glass of sample F2-2. Spinel compositional banding may be quite complex, with cores either being Al- or Cr-rich. Total compositional variation in Cr/(Cr + Al) of cores is 0.227–0.279. Variation in Cr/(Cr + Al) zoning in large spinel is 0.227 (core) to 0.277 (5- to 12-μm-wide light band) to 0.242 (darker, 5-μm outer band) to 0.251 (narrow, 1- to 3-μm-wide rim). Analyses represented are F2-2-19, -20, -21, -22. (**C**) Complexly zoned spinel in microlitic groundmass of F2-1, representing analyses F2-1-27, -28, -29. Spinel contains a Cr-rich core, surrounded sharply by a 3- to 5-μm-wide Al-rich band, which is in turn surrounded by a Cr-rich rim. Zoning represented in Cr/(Cr + Al) is 0.269, 0.220, and 0.232, respectively. (**D**) Skeletal spinel attached to rounded olivine and elongate plagioclase crystals in groundmass of F2-1. Wormy, more aluminous core represents last growth phase of spinel; core and rim analyses are given in Table 3 (F2-1-3, -4). (**E**) Relatively unzoned euhedral spinel in quenched groundmass of olivine dendrites in glass of sample F9-1. Represents analyses F9-1-11, -12 in Table 3. (**F**) Strongly zoned, euhedral spinel and unzoned, skeletal spinel in glass with plagioclase microlites in sample F2-1. Cr-rich core of zoned spinel is rounded, with abrupt transition to aluminous rim. Skeletal spinel is approximately the same composition as the rim of the zoned spinel. Core and rim analyses of the zoned spinel are given in Table 3 (F2-1-7, -8). (**G**) Strongly zoned spinel in glass with feathery plagioclase microlites in sample F2-1. Cr-rich core is rounded, with sharp compositional transition to a skeletal, aluminous rim. Corresponding analyses are given in Table 3 (F2-1-1, -12). (**H**) Sharply zoned spinel in glass, with unzoned, Cr-rich core sharply surrounded by thin (2–15 μm wide) aluminous rim, representing a zoning in Cr/(Cr + Al) of 0.481 to 0.286. Spinel is in sample F2-2 (analyses F2-2-13, -14).

in Figure 4, with compositional ranges given in Table 2. Fe^{3+} content is low (Fe_2O_3 varies from 5.5–9.2%), similar to other spinels from MORBs (Dick and Bullen, 1984; Basaltic Volcanism Study Project, 1981). The low Fe^{3+} content of the spinels reflects the low f_{O_2} of the host Lamont seamount basalts, which range from 1.0 to 1.8 $\log_{10}$ units below the NNO oxygen buffer (calculated using the methods of Sack et al., 1980). This f_{O_2} range is similar to that found in other MORBs by Christie et al. (1986). The compositional range exhibited by the spinels is wide, with Al_2O_3 varying from 22.3 to 47.3%, Cr_2O_3 varying from 18.9 to 39.3%, and MgO varying from 14.5 to 21.4%. The more Al-rich spinels from this seamount group are among the most aluminous spinels reported from MORBs. MgO and Al_2O_3 strongly covary, as do FeO and Cr_2O_3. TiO_2 is a minor component, ranging from 0.16 to 0.85%. Other minor components include NiO (<0.02–0.30%), MnO (0.05–0.47%), CaO (<0.02–0.30%), and SiO_2 (typically <0.1%).

The MgO, FeO, and Al_2O_3 contents of the groundmass spinel rims and of the host glass are strongly correlated (Fig. 5). Sigurdsson and Schilling (1976) found a similar correlation between spinel and host-glass Al content. Strikingly, the Cr_2O_3 content of the spinel is independent of host-glass Cr content (Fig. 5), contrary to the results of Irvine (1976). A difference noted between the ground mass

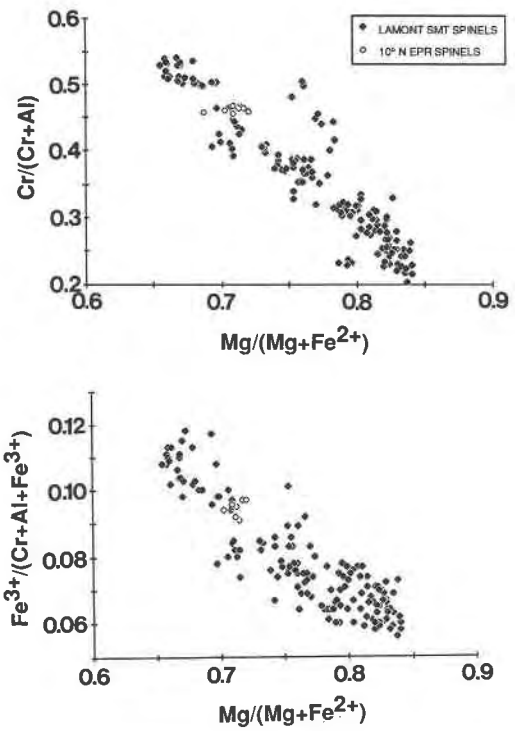

Fig. 4. Composition of Lamont Seamount laval spinels. Spinels are similar in composition to other spinels reported from MORB-type lavas (e.g., Sigurdsson and Schilling, 1976; Sigurdsson, 1977; Basaltic Volcanism Study Project, 1981; Dick and Bullen, 1984). Closed symbols represent spinels from the seamounts and cones; open symbols represent spinels from lavas erupted at the adjacent EPR axis.

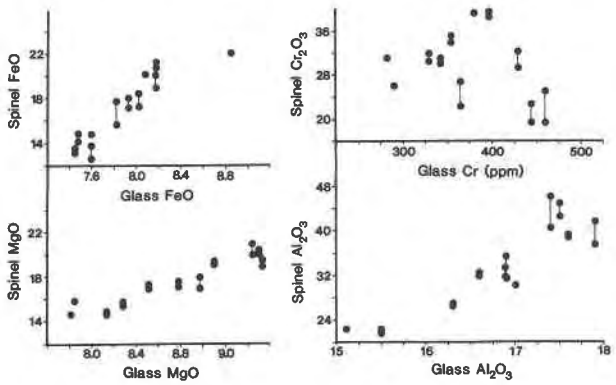

Fig. 5. Comparison of the composition of the rims of groundmass spinels with the composition of the host glass. Connected dots represent the compositional range found within spinels of an individual lava. Note the correlation between spinel and glass MgO, FeO, and Al_2O_3. In contrast, note the poor correlation between host-glass Cr and spinel Cr_2O_3.

spinels and those included within silicate phases is that the rims of the groundmass spinels, on average, are slightly more aluminous and slightly less chromous than those of the included spinels. Figure 6 shows spinels from four lavas of the Lamont seamounts and adjacent EPR, each lava with differing MgO and Al_2O_3 contents. Host-lava MgO and Al_2O_3 contents correlate with the composition of the spinels and result in the sliding of spinel compositions up and down the narrow spinel compositional band of Figure 6.

Most lavas contain only a relatively narrow range of spinel compositions, but in some samples (F2-1, F2-2, F3-4, and 1564-1949) the spinel compositional range is

TABLE 3. Representative spinel analyses

Sample:	1560-1843-1	1560-1843-2	1564-1949-6	1566-1642-1	1566-1642-2	1566-1642-6	1566-1642-7	1567-2019-5	1570-1949-4	1572-1511-6	1572-1511-7	1572-1755-3	F1-1-2B	F2-1-11
Description:*	PC	PR	PC	PC	PR	PC	PR	O	O	GC	GR	PR	GR	GC
SiO_2	0.08	0.10	0.06	0.05	0.06	0.06	0.06	0.07	0.11	0.06	0.09	0.08	0.12	0.06
TiO_2	0.76	0.76	0.37	0.76	0.85	0.75	0.70	0.65	0.45	0.37	0.34	0.49	0.69	0.23
Al_2O_3	29.22	30.15	35.76	23.92	22.28	23.91	24.63	27.58	31.92	37.76	39.02	33.96	23.05	32.30
Cr_2O_3	32.28	30.85	27.51	37.64	38.89	37.41	36.82	34.46	29.66	26.16	25.81	29.72	39.18	34.28
FeO	20.06	20.07	16.70	22.02	21.95	21.12	20.99	19.30	18.36	14.97	14.77	17.15	20.60	14.05
MnO	0.23	0.19	0.08	0.22	0.28	0.23	0.20	0.26	0.11	0.14	0.09	0.00	0.24	0.15
NiO	0.16	0.10	0.13	0.06	0.10	0.09	0.11	0.19	0.18	0.28	0.28	0.00	0.07	0.22
MgO	16.01	15.90	17.73	14.79	14.58	14.91	14.95	16.06	17.43	19.13	19.31	17.68	14.88	18.35
CaO	0.05	0.12	0.08	0.05	0.15	0.07	0.17	0.07	0.19	0.02	0.09	0.17	0.18	0.03
Total	98.85	98.24	98.42	99.51	99.14	98.55	98.63	98.64	98.41	98.89	99.80	99.25	99.01	99.67
FeO**	8.62	8.45	7.10	9.32	9.44	8.94	8.88	8.44	9.16	7.19	6.76	7.27	8.42	5.65
Fe_2O_3**	12.31	12.46	10.31	13.63	13.45	13.07	13.00	11.71	10.12	8.50	8.68	10.60	13.02	8.97
Total**	99.71	99.09	99.13	100.44	100.09	99.45	99.52	99.49	99.33	99.61	100.48	99.98	99.85	100.24
Cr/(Cr + Al)	0.426	0.407	0.340	0.513	0.539	0.512	0.501	0.456	0.384	0.317	0.307	0.370	0.533	0.416
Mg/(Mg + Fe^{2+})	0.699	0.694	0.754	0.659	0.659	0.670	0.672	0.710	0.754	0.800	0.798	0.748	0.671	0.785
Fe^{3+}/(Cr + Al + Fe^{3+})	0.098	0.096	0.077	0.108	0.111	0.104	0.103	0.096	0.101	0.077	0.071	0.079	0.098	0.061

* C refers to spinel core, R refers to spinel rim, P refers to spinel included in plagioclase, O refers to spinel included in olivine, and G refers to spinel found in the groundmass.

**Recalculation of FeO and Fe_2O_3 after Carmichael (1967), based on stoichiometry.

much broader (Table 2). Similarly, compositional zoning in the spinels of most lavas is minor (for example, 1560-1843-1, -2; 1566-1642-1, -2; 1566-1642-6, -7; 1572-1511-6, -7; and F9 1-11, -12 in Table 3). Nevertheless, zoning of some spinels within samples F2-1 and F2-2 is strongly developed (Figs. 3 and 10), with zoning parallel to the Cr/(Cr + Al) vs. Mg/(Mg + Fe^{2+}) compositional trend of Figures 4 and 6 and typically progressing from a core with higher Cr/(Cr + Al) and lower Mg/(Mg + Fe^{2+}) to a rim with a lower Cr/(Cr + Al) and a higher Mg/(Mg + Fe^{2+}). For the strongly zoned spinels, the zoning is typically quite abrupt; most strongly zoned spinels contain a rounded, Cr-rich core surrounded by an Al-rich rim that may have either skeletal or euhedral outlines. The spinel compositional trends are crystal-chemically controlled and reflect the strongly coupled substitutions of Mg^{2+} and Al^{3+} and of Fe^{2+} and Cr^{3+} into the spinel structure (e.g., Sack, 1982; Hill and Sack, 1987; Engi, 1983). These well-developed zoning trends are distinct from other spinel crystallization trends predicted (Dick and Bullen, 1984) or experimentally observed (Fisk and Bence, 1980; Irvine, 1976; Sack, 1982) for spinels coprecipitating with olivine or plagioclase or both.

Complex compositional zoning occurs in some spinels of F2-1 and F2-2, but is generally only of limited compositional range (Figs. 3 and 10). Compositional bands may be quite narrow (1 μm or larger), and cores may be either relatively Cr- or Al-rich.

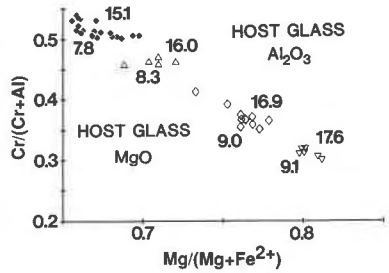

Fig. 6. Spinel compositions plotted from four lavas erupted from the Lamont seamounts, showing generally how host-lava composition affects spinel composition. Different symbols represent spinels from different individual lavas, with host-lava MgO below and host-lava Al_2O_3 above the corresponding spinels. Symbols representing spinel compositions are the same as in Fig. 7, with solid diamonds representing spinels from 1566-1642; open triangles, from 1567-2019; open diamonds, from F9-1; and upside down, open triangles, from 1572-1511. Note how changing host-lava Al_2O_3 and MgO slides the spinel composition up and down the narrow spinel composition band.

Discussion

Spinel compositional systematics

Despite the complexity of spinel zoning patterns in some of the Lamont seamount lavas, most have spinels that exhibit only limited variability in Cr/Al and Fe^{3+}/Al ratios. These display simple Fe^{2+}-Mg zoning patterns that may be related to fractionation of the lavas and to interlava compositional variations that are largely crystal-chemically controlled. Both of these points are readily illustrated with a plot that makes provision for crystal-chemical effects on the Fe^{2+}-Mg exchange reaction between spinel and host silicate liquid. We assume that spinel behaves as an ideal reciprocal solution (e.g., Wood and Nicholls, 1978; Sack, 1982) and that silicate liquids are ideal with respect to mixing of Fe^{2+} and Mg^{2+}. In

TABLE 3—*Continued*

F2-1-12 GR	F2-1-2 G	F2-1-3 GC	F2-1-4 GR	F2-1-7 GC	F2-1-8 GR	F2-2-10 OC	F2-2-11 OR	F2-2-19 GC	F2-2-24 OC	F2-2-25 OR	F3-4-12 PC	F3-4-18 G	F9-1-11 GC	F9-1-12 GR
0.10	0.06	0.09	0.15	0.12	0.10	0.08	0.09	0.09	0.08	0.06	0.08	0.10	0.10	0.14
0.21	0.37	0.15	0.22	0.28	0.26	0.39	0.31	0.16	0.73	0.56	0.38	0.28	0.46	0.44
45.85	26.42	47.21	42.90	37.57	43.48	38.70	42.79	45.35	25.73	29.21	27.91	38.07	35.33	34.08
18.94	39.15	17.88	21.84	28.30	20.57	25.82	21.57	19.81	39.30	35.32	35.98	26.72	30.02	30.12
12.76	14.56	12.06	13.15	13.50	13.65	13.91	13.48	12.11	15.67	14.83	18.36	14.23	14.81	16.51
0.17	0.22	0.08	0.16	0.17	0.16	0.18	0.15	0.10	0.15	0.18	0.28	0.14	0.06	0.15
0.24	0.10	0.33	0.24	0.22	0.28	0.29	0.19	0.31	0.26	0.13	0.12	0.27	0.24	0.24
20.70	17.09	20.80	19.95	19.27	20.14	19.62	20.29	20.75	17.39	17.68	15.74	18.92	18.60	17.97
0.10	0.16	0.05	0.13	0.07	0.13	0.03	0.08	0.00	0.04	0.01	0.09	0.06	0.04	0.10
99.07	98.13	98.65	98.74	99.50	98.77	99.02	98.95	98.68	99.35	97.98	98.94	98.79	99.66	99.75
6.14	5.63	5.47	5.89	5.68	6.71	6.67	6.63	5.67	6.59	6.09	6.94	6.09	6.03	7.16
7.23	9.49	7.14	7.85	8.39	7.61	7.91	7.52	7.01	9.74	9.35	12.11	8.75	9.38	10.07
99.69	98.69	99.20	99.33	100.07	99.44	99.69	99.61	99.25	100.01	98.59	99.64	99.40	100.26	100.47
0.217	0.498	0.203	0.254	0.336	0.241	0.309	0.253	0.227	0.506	0.448	0.464	0.320	0.363	0.372
0.836	0.762	0.838	0.819	0.804	0.825	0.815	0.828	0.841	0.761	0.771	0.698	0.794	0.779	0.761
0.063	0.064	0.056	0.061	0.060	0.070	0.071	0.069	0.058	0.075	0.068	0.078	0.065	0.065	0.078

addition, we assume that the pressure effect over the spinel crystallization range on spinel composition is relatively small compared to the effect of varying the host-lava composition, and so may be neglected. For these assumptions we may write the following expression for the Fe-Mg exchange reaction between spinel and silicate liquid:

$$\ln K_D^{sp\text{-}liq} = -\frac{\Delta\bar{G}^0_{ex}}{RT} + \frac{\Delta\mu^0_{23}}{RT}(X_3) + \frac{\Delta\mu^0_{24}}{RT}(X_4) + \frac{\Delta\mu^0_{25}}{RT}(X_5), \quad (1)$$

where

$$\Delta\bar{G}^0_{ex} = (\bar{G}^0_{MgO} - \bar{G}^0_{FeO})^{liq} + (\bar{G}^0_{FeAl_2O_4} - \bar{G}^0_{MgAl_2O_4})^{sp},$$

$$\Delta\mu^0_{23} = (\bar{G}^0_{MgCr_2O_4} + \bar{G}^0_{FeAl_2O_4})^{sp} - (\bar{G}^0_{FeCr_2O_4} + \bar{G}^0_{MgAl_2O_4})^{sp},$$

$$\Delta\mu^0_{24} = (\tfrac{1}{2}\bar{G}^0_{Mg_2TiO_4} + \bar{G}^0_{FeAl_2O_4})^{sp} - (\tfrac{1}{2}\bar{G}^0_{Fe_2TiO_4} + \bar{G}^0_{MgAl_2O_4})^{sp},$$

$$\Delta\mu^0_{25} = (\bar{G}^0_{MgFe_2O_4} + \bar{G}^0_{FeAl_2O_4})^{sp} - (\bar{G}^0_{Fe_3O_4} + \bar{G}^0_{MgAl_2O_4})^{sp},$$

$$X_3 = \tfrac{1}{2}n^{sp}_{Cr^{3+}},\ X_4 = n^{sp}_{Ti^{4+}},\ X_5 = \tfrac{1}{2}n^{sp}_{Fe^{3+}},$$

and the n_i terms are the number of the i cations in a formula unit based on three cations (e.g., Sack, 1982; Hill and Sack, 1987).

In a first approximation suitable for illustration, several simplifications of Equation 1 may be made. First, because Ti^{4+} is negligible in the Lamont seamount spinels, we will ignore the third term on the right-hand side of Equation 1. Second, we approximate that $\Delta\mu^0_{25} = \frac{4}{3}\Delta\mu^0_{23}$, where $\Delta\mu^0_{23} = 4.80$ kcal/gfw and $\Delta\mu^0_{25} = 6.39$ kcal/gfw, as established by Hill and Sack (1987). Making these modifications reduces Equation 1 to

$$\ln K_D^{sp\text{-}liq} = -\Delta\bar{G}^0_{ex}/RT + (4.80/RT)(Y), \quad (2)$$

where $Y = X_3 + \frac{4}{3}(X_5)$. We note that Y and Cr/(Cr + Al) are essentially equivalent for spinels within a given sample, because of the minor variation of Fe^{3+}.

Spinel compositions from the 11 lava samples exhibiting limited spinel compositional range and little spinel zoning are plotted in Figure 7 using these parameters. These spinels define a crystal-chemical trend with positive slope, with spinels from more primitive, MgO- and Al_2O_3-rich lavas plotting at lower values of ln K_D and Y and spinels from more evolved lavas plotting at the higher ln K_D and Y values in the trend. These results show that the Cr-rich spinels in this study become progressively more Cr-rich as the host lava becomes more fractionated. This trend is due to the reciprocal exchange substitution of Cr and Fe^{2+} for Mg and Al in the spinel. Olivine and plagioclase fractionation will cause magmatic Fe^{2+} to increase and magmatic Al and Mg to decrease, resulting in the crystallization of spinels higher in Cr/(Cr + Al) and lower in Mg/(Mg + Fe^{2+}). This correlation between spinel composition and degree of fractionation of the host lava is strikingly shown by comparing the Cr/(Cr + Al) ratio or the quantity Y in the spinels with the normative ratio Di/(Ol + Di) of the host glasses (Fig. 8). The independence of spinel and glass Cr contents may reflect the paucity of Cr in the melt.

Finally, we may estimate an approximate value for $-\Delta G^0_{ex}$ from the FeO/MgO ratios of the glass chemical analyses, from Equation 2, and from the compositions of the rims of groundmass spinels (to insure approximation of crystal-liquid equilibria). To do so we assume (1) that spinel is the first phase to crystallize from the lavas (e.g., Sack et al., 1987, and from petrographic observations); (2) that spinels do not exhibit retrograde Fe-Mg exchange during crystallization (unlikely because of quick magmatic quench after eruption on the ocean floor); (3) and an average temperature of initial crystallization of 1200 °C (derived from olivine-liquid geothermometry based on Glazner, 1984). From the values of ln $K_D^{sp\text{-}liq}$ calculated by employing these assumptions, we obtain an estimate for $-\Delta G^0_{ex}$ of -3.40 ± 0.18 kcal/gfw. This value for $-\Delta G^0_{ex}$ is slightly smaller than that (-3.16 ± 0.11 kcal/gfw) which may be calculated fom the calibration of Hill and Sack (1987) for ln $K_D^{ol\text{-}sp}$, using the average values of $X^{ol}_{Mg_2SiO_4}$ and $(X^{glass}_{MgO}/X^{glass}_{FeO})$ $(X^{ol}_{Fe_2SiO_4}/X^{ol}_{Mg_2SiO_4})$ of 0.878 and 0.267 ± 0.008, respectively, as determined for the Lamont seamount lavas by microprobe analysis. Nevertheless, these estimates are within analytical error of each other, indicating that the calibration of Hill and Sack (1987) is essentially correct. We use the former estimate of -3.40 ± 0.18 kcal/gfw to calibrate the correlation for Equation 2 plotted in Figure 7 for illustrative purposes.

The compositions of spinels within lavas exhibiting limited spinel compositional range essentially agree with the crystal-chemical trend as defined by Equation 2. Spinels in these lavas exhibit some variation in ln[(MgO/FeO)^{glass}(Fe^{2+}/Mg^{2+})^{spinel}], which perhaps could be attributed to limited coprecipitation with olivine. The earlier-crystallizing spinels that have not fully re-equilibrated with the evolving host liquid will define more negative ln K_D values at a given Y.

Spinel zoning and its petrogenetic implications

We now use these observations to examine more closely the Lamont seamount spinels exhibiting strong zoning, complex zoning, or extensive compositional variation within an individual sample. Spinels from the four Lamont seamount lavas (F2-1, F2-2, F3-4, and 1564-1949) that exhibit wide compositional variation are plotted in Figure 9 in terms of the parameters defined in Equation 2. Selected examples of spinel zoning are presented in Figure 10.

Lava samples F2-1 and F2-2 contain two types of olivine phenocrysts—skeletal, unzoned olivines of $Fo_{89\text{–}90}$ composition, and subhedral-euhedral, reversely zoned olivines with $Fo_{87\text{–}88}$ cores and $Fo_{89\text{–}90}$ rims. As illustrated in Figure 9, the spinels in these samples span a broad compositional range, containing spinels strongly zoned in Cr/(Cr + Al) (F2-1-7, -8; F2-1-11, -12; and F2-2-13, -14 in Figs. 3 and 10). The rounded, resorbed-appearing cores

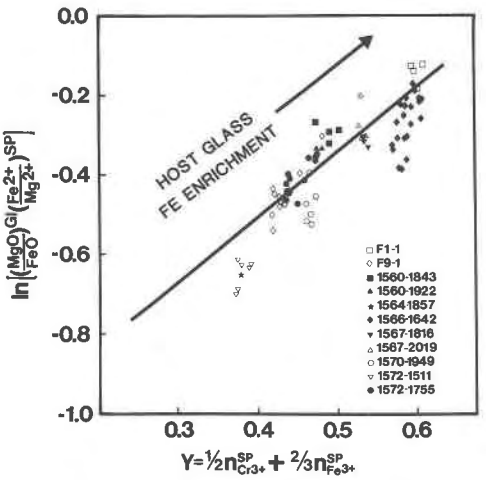

Fig. 7. Compositions of spinels from lavas with spinels exhibiting restricted compositional ranges, plotted in terms of ln·($K_D^{sp\text{-}liq}$) vs. Y, where $Y = \frac{1}{2}n^{sp}_{Cr3+} + \frac{2}{3}n^{sp}_{Fe3+} = X_3 + \frac{4}{3}X_5$ (n_i indicates the i^{th} cation calculated on a three-cation basis). Note that MgO and FeO in the axis label refers to the molecular equivalents of these oxides. The solid line represents the calibration of Equation 2 given in the text by the rim compositions of groundmass spinels. The spinels from these 11 lavas define a simple, straightforward crystal-chemical trend, reflecting equilibria between the spinels and their host silicate liquid. Spinels with higher values of Y (those richer in Cr) are associated with more evolved magmas richer in Fe. See text for further discussion.

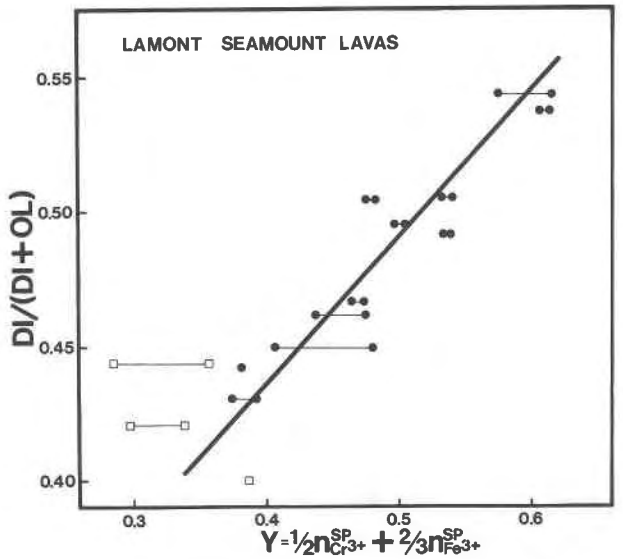

Fig. 8. Comparison of the range in value of Y for spinels in individual lavas with the normative Ol/(Ol + Di) ratio of the host glass calculated from the algorithms of Sack et al. (1987). Dots represent the range in spinels of the 11 lavas where the spinel compositional range is small, as shown in Fig. 7. Open squares represent the range in composition of the rims of groundmass spinels in the four lavas where the range in spinel composition is large, as shown in Fig. 9. Diagonal line represents an approximate fit to the data.

of the zoned spinels are Cr-rich and sharply bounded by skeletal Al-rich rims. The Al-rich rims are similar in composition to that of the bulk of the spinels found within these lavas and are in apparent equilibrium with the host glass. In contrast, the Cr-rich spinel compositions likely crystallized from a liquid considerably more evolved and Fe-rich than the host glass. As shown in Figure 10, the Cr-rich spinels (high in Y) included within olivines are found within Fo_{87} olivine cores, whereas the Al-rich spinels included in olivine are found within skeletal Fo_{89-90} olivines. These more Cr-rich spinels in the Fo_{87} olivines are similar in composition to other Lamont seamount groundmass spinels found within other lavas that crystallized Fo_{87} olivine.

Other Cr-rich spinels from F2-1 and F3-4 are found within plagioclase phenocrysts that presumably armored them from interaction with the host liquid. They are considerably less aluminous than other spinels found in the groundmass and in apparent equilibrium with the host glass. The Cr-rich spinels in F3-4 are found as inclusions within the core of a single large plagioclase phenocryst that shows simple reverse zoning from An_{86} to An_{90} midway from core to rim. The core of this crystal also contains an inclusion of Fo_{87} olivine, whereas the other olivines of this sample are Fo_{89-90} in composition. Again, the Cr-rich spinels in this sample are similar in composition to spinels crystallizing from other lavas in this suite that crystallized Fo_{87} olivines. Sample 1564-1949 contains a compositionally diverse population of spinels as well, yet its silicate mineralogy is more diverse than that of other samples with complex spinel populations. Besides containing slight reverse zoning in many of its olivine phenocrysts, its plagioclase phenocrysts are reversely and complexly zoned (up to An_{13}).

The Cr-rich spinels in F2-1, F2-2, F3-4, and 1564-1949 were likely introduced externally into the rising magma, having crystallized from melts more evolved and Fe-rich than the lavas in which they are found. Nevertheless, the lack of xenoliths, the primitiveness of the host glasses, the lack of clinopyroxene, and the lack of significant zoning in most olivines and in the feldspars of all lavas except 1564-1949 argue that processes such as magma mixing or crustal assimilation were of minor significance in the evolution of these lavas. The range in spinel composition probably reflects magma mixing during the periodic refilling of small crustal or edifice magma chambers just prior to eruption, where the magma residence time is short and the fractionation minimal. The skeletal nature of some of the Al-rich spinels may represent rapid growth triggered by magma mixing, on the basis of the concave curvature of the experimental basalt liquidus surfaces away from the spinel field (Dick and Bullen, 1984; Irvine, 1977). Viewed this way, the composition of the Cr-rich spinels provide qualitative limits for determining the compositions of the end-member liquids being mixed.

Several of the groundmass spinels within samples F2-1

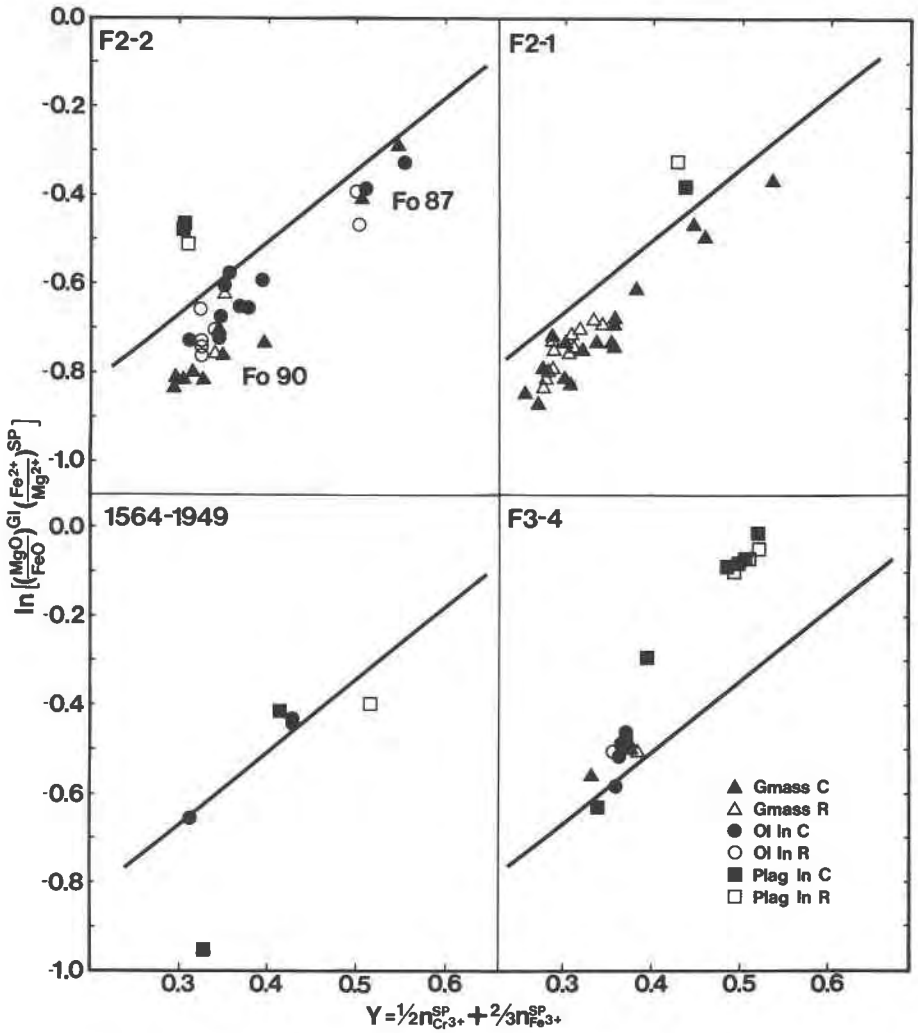

Fig. 9. Spinels from the lavas of the Lamont seamount group exhibiting wide variation in spinel composition, plotted as in Fig. 8. Closed symbols refer to spinel cores and open symbols refer to spinel rims; triangles represent groundmass spinels; circles represent spinels included in olivine; and squares represent spinels included in plagioclase. Reference lines representing the calibration of Equation 2 and shown in Fig. 8 are also given here. Note that the F2-2 spinels high in Y and included in olivine are found within Fo_{87} cores of olivine reversely zoned to Fo_{90} composition, whereas the low-Y spinels included in olivine are found within skeletal olivine phenocrysts of Fo_{90} composition. See text for further discussion.

and F2-2 contain minor complex zoning (F2-1-27, -28, -29 and F2-2-19, -20, -21, -22; Figs. 3 and 10). The compositional range represented by this zoning falls within the range outlined by the rims of other groundmass spinels found in these lavas. Therefore, it is not necessary to invoke magma mixing or assimilation to account for this zoning; rather, it may be related to local melt depletion in Cr from rapid spinel crystallization (Thy, 1983; Allan et al., 1987) with subsequent transportation of the spinel to more Cr-rich portions of the magma body. One curious spinel within F2-1 (F2-1-3, -4; Fig. 3, Table 3) consists of a skeletal, Al-rich rim (42.9% Al_2O_3) with an anhedral, wormy core representing not only the most aluminous composition (47.2% Al_2O_3) in the entire suite but presumably the last portion of the spinel to crystallize. The compositional zoning represented within this spinel seems rather large to be related to local melt depletion in Cr, and the origin of its zoning remains somewhat enigmatic.

Comments on spinel as a possible indicator of pressure

Although all of the strongly zoned spinels examined have Cr-rich cores, it is likely that Al-rich cores of strongly zoned spinels may also result from magma mixing or assimilation. Sigurdsson (1977) has reported "reversely" zoned spinels from DSDP Hole 332B plagioclase-phyric basalts that may represent just such a case. These spinels

contain highly aluminous cores with sharp increases of Cr/(Cr + Al) and decreases of Mg/(Mg + Fe^{2+}) from core to rim. Other authors (Sigurdsson and Schilling, 1976; Dick and Bryan, 1978; Dick and Bullen, 1984) have found unzoned high-Al spinels in picritic lavas. Both zoned and unzoned high-Al spinels, similar in Al content to the more aluminous of the Lamont seamount spinels, were previously interpreted as representing high-pressure relicts, on the basis of (1) scant experimental evidence that the Al content of spinels increases with pressure (Green et al., 1971; Jaques and Green, 1979; P. Roeder, pers. comm., 1987) and (2) the observation that spinels in lherzolite nodules are typically aluminous. Dick and Bullen (1984) suggested that pressure may affect spinel composition by changing the melt/spinel partitioning coefficient for Cr, because of increased octahedral melt sites with pressure resulting in increased Cr solubility in the melt.

The presence of Al-rich, skeletal rims of groundmass spinels surrounding Cr-rich spinel cores in the Lamont seamount lavas clearly shows that Cr-spinel with Cr/(Cr + Al) as low as 0.2 can crystallize at low pressures. We therefore believe that the presence of Al-rich spinels in MORBs may not represent high-pressure processes but may instead reflect low-pressure equilibrium crystallization, magma mixing, or wallrock assimilation. Although more experimental work is needed to determine whether solubility of Cr-rich minerals in melt appreciably changes over the pressures of interest, we wish to note that the difference in the 1-bar molar volumes between $FeCr_2O_4$ (chromite) and $MgAl_2O_4$ (spinel) is on the order of 10% (4.4010 vs. 3.9710 J/bar, respectively; Robie et al., 1978). The compositional effect of the ΔV of the exchange equation

$$(MgAl_2O_4)^{sp} + (FeCr_2O_4)^{liq} \rightleftharpoons (FeCr_2O_4)^{sp} + (MgAl_2O_4)^{liq} \quad (3)$$

is likely small, when compared to the very large differences in spinel composition [i.e., Cr/(Cr + Al) variation of 0.2–0.54] caused by the minor variations in host-lava composition as seen in the Lamont seamount lavas. This observation implies that a quantitative geobarometer based on spinel-liquid exchange may be a difficult problem to implement, because of the difficulty of separating pressure effects from compositional effects.

Conclusions

1. Cr-rich spinels from the near-ridge Lamont seamounts and from the adjacent EPR crest at 10°N occur in lavas that contain greater than 260 ppm Cr and that have Mg/(Mg + Fe^{2+}) greater than 0.61.

2. These Cr-rich spinels vary systematically in composition with host-lava composition and "primitiveness," as measured either by normative Ol/(Ol + Diop) ratios or Mg/(Mg + Fe^{2+}), with spinels richer in Cr- and Fe^{2+} crystallizing from the more evolved lavas.

3. Recasting of spinel compositions in terms of thermodynamically relevant components representing exchange reactions allows the determination of whether Cr-rich spinels are in equilibrium with the host liquid. Specific examples given here show that large ranges in spinel Cr/(Cr + Al) content within a given lava reflect incorporation of xenocrystal spinels that crystallized from a silicate liquid of different Mg/(Mg + Fe^{2+}) content than the host magma and likely reflect magma mixing in a shallow magma chamber just prior to eruption.

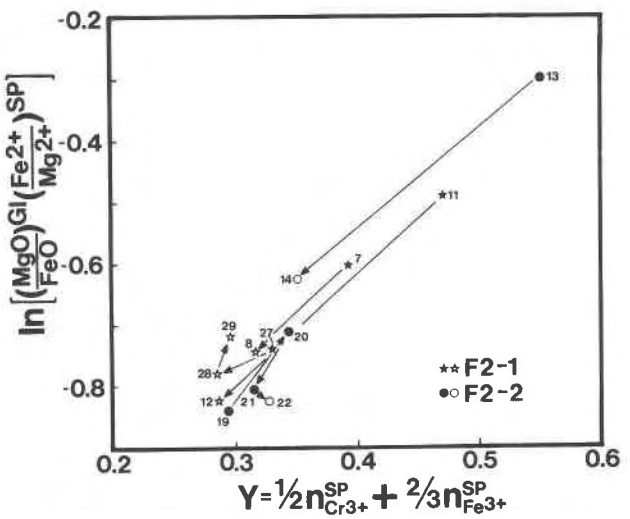

Fig. 10. Compositional zoning in selected strongly zoned or complexly zoned spinels from the groundmass of F2-1 (stars) and F2-2 (circles); interiors of spinels are shown by solid symbols, and spinel rims are shown by open symbols. Arrows indicate direction of core to rim, and the analyses numbers are also given for reference.

4. Al-rich (to over 47% Al_2O_3 by weight) groundmass spinels and skeletal groundmass rims in "primitive" lavas clearly show that Al-rich spinels crystallize at low pressure and that Al-rich cores of reversely zoned spinels may in some cases represent magma mixing or wallrock assimilation rather than represent high-pressure relicts (e.g., Sigurdsson, 1977).

5. The Cr content of spinels within a given lava has little relationship to host-liquid Cr content. Instead, spinel Cr is indirectly controlled by the host-lava Al, Fe^{2+}, and Mg contents through reciprocal exchange reactions in a manner that is qualitatively but not yet quantitatively predictable. This observation, coupled with the observation that these elements in spinel (particularly Al) strongly covary with small changes in host-liquid composition, indicates that quantitative use of Cr-rich spinels as geobarometers will be a difficult problem to implement. Nevertheless, these same observations show that Cr-rich spinels are powerful petrogenetic tools for providing information about interaction between silicate liquids or silicate liquids and solids.

Acknowledgments

Host lavas for the spinels were collected during the Clipperton (1985) expedition; we are indebted to chief scientist D. Fornari, the crew of the

Atlantis II, and to the *ALVIN* pilots and crew. We are grateful to F. Bishop, P. Roeder, H. Sigurdsson, and J. A. Speer for reviewing the manuscript and to F. Bishop and B. Wood for providing numerous suggestions regarding the petrological and geochemical significance of variations in spinel chemistry. J.F.A. also thanks G. Adams, I. Carmichael, P. Castillo, H. Dick, M. Fisk, R. Loucks, G. Mattioli, J. Natland, J. Pasteris, and M. Perfit for compelling discussions concerning this research and D. Kremser for analytic assistance on the electron microprobe. We thank W. Melson and T. O'Hearn for providing the glass major-elemental analyses and I. Carmichael and D. Christie for the glass FeO analyses. This work was supported by NSF grants OCE-8308980, OCE-8415270, and OCE-8508042 (R. Batiza), ONR grant 10-14-80-C-0856 (R. Batiza), NSF grant EAR-8419158 (R. O. Sack), and NSF grant OCE-8414616 (D. Fornari), with support to J.F.A. during revision of the paper from NSERC Strategic Operating Grant 5-55847 (R. Chase).

References cited

Allan, J.F., Batiza, R., Perfit, M., and Fornari, D. (1986) Extremely depleted basalts from seamounts near the EPR (9°53′N): Evidence for continued melting during outward lateral transport of sub-axial upper mantle (abs.). EOS, 67, 1184.

Allan, J.F., Batiza, R., and Lonsdale, P. (1987) Petrology of lavas from seamounts flanking the East Pacific Rise axis, 21°N: Implications concerning the mantle source composition for both seamount and adjacent EPR lavas. In B. Keating, I. Fryer, and R. Batiza, Eds., Seamounts, islands, and atolls. American Geophysical Union Geophysical Monograph 43, 255–282.

Basaltic Volcanism Study Project (1981) Basaltic volcanism on the terrestrial planets. Pergamon Press, New York.

Batiza, R., and Vanko, D. (1984) Petrology of young Pacific seamounts. Journal of Geophysical Research, 89, 11235–11260.

Byerly, G.R., Melson, W.G., Nelen, J.A., and Jarosewich, E. (1976) Abyssal basaltic glasses as indicators of magma compositions. In B. Mason, Ed., Mineral science investigations, 1974–1975. Smithsonian Contributions to the Earth Sciences, 19, 22–30.

Carmichael, I.S.E. (1967) The iron-titanium oxides of salic volcanic rocks and their associated ferromagnesian silicates. Contributions to Mineralogy and Petrology, 14, 36–64.

Christie, D.M., Carmichael, I.S.E., and Langmuir, C.H. (1986) Oxidation states of mid-ocean ridge basalt glasses. Earth and Planetary Science Letters, 79, 397–411.

Detrick, P.S., Buhl, P., Vera, E., Mutter, J., Madsen, I., and Brocher, T. (1987) Multi-channel seismic imaging of a crustal magma chamber along the East Pacific Rise. Nature, 326, 35–41.

Dick, H.J.B., and Bryan, W.B. (1978) Variation of basalt phenocryst mineralogy and rock compositions in DSDP hole 396B. Initial Reports of the Deep Sea Drilling Project, 46, 215–225.

Dick, H.J.B., and Bullen, T. (1984) Chromium spinel as a petrogenetic indicator in abyssal and alpine-type peridotites and spatially associated lavas. Contributions to Mineralogy and Petrology, 86, 54–76.

Engi, M. (1983) Equilibria involving Al-Cr spinel: Mg-Fe exchange with olivine. Experiments, thermodynamic analysis, and consequences for geothermometry. American Journal of Science, 283-A, 29–71.

Fisk, M.R., and Bence, A.E. (1980) Experimental crystallization of chrome spinel in FAMOUS basalt 527-1-1. Earth and Planetary Science Letters, 48, 111–123.

Fornari, D.J., Ryan, W.B.F., and Fox, P.J. (1984) The evolution of craters and calderas on young seamounts. Insights from SEA MARC I and SEA BEAM sonar surveys of a small seamount group near the axis of the East Pacific Rise at ≈ 10°N. Journal of Geophysical Research, 89, 11069–11083.

Fornari, D., Perfit, M., Allan, J., Batiza, R., Haymon, R., Barone, A., Ryan, W.B.F., Smith, T., and Simkin, T. (1988a) Seamounts as windows into mantle processes: Structural and geochemical studies of the Lamont seamounts. Earth and Planetary Science Letters, in press.

Fornari, D., Perfit, M., Allan, J., and Batiza, R. (1988b) Small-scale heterogeneities in depleted mantle sources: Near-ridge seamount lava geochemistry and implications for ocean ridge magmatic processes. Nature, 331, 511–513.

Foruta, T., and Tokuyama, H. (1983) Chromium spinels in Costa Rica basalts, Deep Sea Drilling Project Site 505—A preliminary interpretation of electron microprobe analyses. Initial Reports of the Deep Sea Drilling Project, 69, 805–810.

Frey, F.A., Green, D.H., and Roy, S.D. (1978) Integrated models of basalt petrogenesis: A study of quartz tholeiites to olivine melilites from southeast Australia utilizing geochemical and experimental petrologic data. Journal of Petrology, 19, 463–513.

Gallo, D.G., Fox, J., and Macdonald, K.C. (1986) A sea beam investigation of the Clipperton transform fault. The morphotectonic expression of a fast slipping transform boundary. Journal of Geophysical Research, 91, 3455–3467.

Glazner, A.F. (1984) Activities of olivine and plagioclase components in silicate melts and their application to geothermometry. Contributions to Mineralogy and Petrology, 88, 260–268.

Green, D.H. (1971) Compositions of basaltic magmas as indicators of conditions of origin: Application to oceanic volcanism. Philisophical Transactions of the Royal Society of London, ser. A, 268, 707–725.

Green, D.H., Ringwood, A.E., Ware, N.G., Hibberson, W.O., Major, A., and Kiss, E. (1971) Experimental petrology and petrogenesis of Apollo 12 basalts. Proceedings of the Second Lunar Science Conference, 1, 601–615.

Haskin, L.A., Wildeman, T.R., and Haskin, M.A. (1968) An accurate procedure for the determination of the rare earths by neutron activation. Journal of Radioanalytic Chemistry, 1, 337–348.

Hill, R.L., and Sack, R.O. (1987) Thermodynamic properties of Fe-Mg titanomagnetite spinels. Canadian Mineralogist, 25, 443–464.

Irvine, T.N. (1965) Chrome spinel as a petrogenetic indicator, 1, Theory. Canadian Journal of the Earth Sciences, 2, 648–672.

——— (1967) Chromium spinel as a petrogenetic indicator: Part 2, Petrological applications. Canadian Journal of the Earth Sciences, 4, 71–103.

——— (1976) Chromite crystallization in the join Mg_2SiO_4-$CaMgSi_2O_6$-$CaAl_2Si_2O_8$-$MgCr_2O_4$-SiO_2. Carnegie Institution of Washington Year Book 76, 465–472.

——— (1977) Origin of chromitite layers in the Muskox intrusion and other stratiform intrusions: A new interpretation. Geology, 5, 273–277.

Jaques, A.L., and Green, D.H. (1979) Anhydrous melting of peridotite at 0–15 kb pressure and the genesis of tholeiitic basalts. Contributions to Mineralogy and Petrology, 73, 287–310.

Kastens, K.A., Ryan, W.B.F., and Fox, J. (1986) Structural and volcanic expression of a fast slipping ridge-transform boundary: Sea MARC I and photographic surveys at the Clipperton transform fault. Journal of Geophysical Research, 91, 3469–3488.

Klein, E., Langmuir, C., Bender, J., Batiza, R., and Zindler, A. (1986) Nd and Sr isotopic composition of volcanic glasses from the East Pacific Rise (8°N–12°N). EOS, 67, 1255.

Langmuir, C.H., Bender, J.F., and Batiza, R. (1986) Petrological and tectonic segmentation of the East Pacific Rise, 5°30′–14°30′N. Nature, 322, 422–429.

Melson, W.G., Vallier, T.L., Wright, T.L., Byerly, G., and Nelen, J. (1976) Chemical diversity of abyssal volcanic glass erupted along Pacific, Atlantic, and Indian Ocean sea-floor spreading centers. In G.H. Sutton, M.H. Manghnani, and R. Moberly, Eds., The geophysics of the Pacific Ocean basin and its margin, American Geophysical Union Geophysical Monograph 19, 351–367.

Natland, J.H., Adamson, A.C., Laverne, C., Melson, W.G., and O'Hearn, T. (1983) A compositionally nearly steady-state magma chamber at the Costa Rica Rift: Evidence from basalt glass and mineral data. Deep Sea Drilling Project Sites 501, 504, and 505, Initial Reports of the Deep Sea Drilling Project, 69, 811–858.

Perfit, M.R., Shuster, R.D., Allan, J., Batiza, R., and Fornari, D. (1986) Trace element and isotopic characteristics of seamounts near the East Pacific Rise. Probes to MORB sources: EOS, 67, 1184.

Presnall, D.C., Dixon, J.R., O'Donnell, T.H., and Hoover, J.D. (1979) Compositions and depth of origin of primary mid-ocean ridge basalts. Journal of Petrology, 20, 3–35.

Rhodes, J.M., and Dungan, M.A. (1979) The evolution of ocean-floor basaltic magmas: Deep drilling results in the Atlantic Ocean. American Geophysical Union Maurice Ewing Series, 2, 262–272.

Robie, R.A., Hemingway, B.S., and Fisher, J.R. (1978) Thermodynamic properties of minerals and related substances at 298.15 K and 1 bar

(10^5 pascals) pressure and at higher temperatures. U.S. Geological Survey Bulletin 1452.

Sack, R.O. (1982) Spinels as petrogenetic indicators: Activity-composition relations at low pressures. Contributions to Mineralogy and Petrology, 79, 169–186.

Sack, R.O., Carmichael, I.S.E., Rivers, M.L., and Ghiorso, M.S. (1980) Ferric-ferrous equilibria in natural silicate liquids at 1 bar. Contributions to Mineralogy and Petrology, 75, 369–376.

Sack, R.O., Walker, D., and Carmichael, I.S.E. (1987) Experimental petrology of alkaline lavas: Constraints on cotectics of multiple saturation in natural basic liquids. Contributions to Mineralogy and Petrology, 96, 1–23.

Sato, H. (1977) Nickel content of basaltic magmas: Identification of primary magmas and a measure of the degree of olivine fractionation. Lithos, 10, 113–120.

Sempere, J.-C., and Macdonald, K.C. (1986) Deep-tow studies of the overlapping spreading centers at 9°03′N on the East Pacific Rise. Tectonics, 5, 881–900.

Sigurdsson, H. (1977) Spinels in leg 37 basalts and peridotites: Phase chemistry and zoning. Initial Reports of the Deep Sea Drilling Project, 37, 883–891.

Sigurdsson, H., and Schilling, J.-G. (1976) Spinels in Mid-Atlantic Ridge basalts: Chemistry and occurrence. Earth and Planetary Science Letters, 29, 7–20.

Sun, S.S., Nesbitt, R.W., and Sharaskin, A.Y. (1979) Geochemical characteristics of mid-ocean ridge basalts. Earth and Planetary Science Letters, 44, 119–138.

Thy, P. (1983) Spinel minerals in transitional and alkalic basaltic glasses. Contributions to Mineralogy and Petrology, 83, 141–149.

Walker, D., Shibata, T., and DeLong, S.E. (1979) Abyssal tholeiites from the Oceanographer Fracture Zone, II, Phase-equilibria and mixing. Contributions to Mineralogy and Petrology, 70, 111–125.

Wood, B.J., and Nicholls, J. (1978) The thermodynamic properties of reciprocal solid solutions. Contributions to Mineralogy and Petrology, 66, 389–400.

Manuscript received June 29, 1987
Manuscript accepted March 9, 1988